We_Dome3_02

Field Test Results of a Novel Low-Frequency Marine Source

S. Chelminski[2], F. Chelminski[2], J. Chelminski[2], F. Lam[3], S. Ronen[2,3], G. Baeten[1], D. Chavan[1]*, B. Kuvshinov[1], F. Ten Kroode[1]

[1] Shell International E&P BV; [2] Low Impact Seismic Sources; [3] Stanford University

Summary

We have tested a new marine source whose initial volume of up to 100 times the volume of a conventional airgun produces low-frequency bubble oscillations with a resonance in the order of 3 Hz. The resulting improvement in low frequency output is in the order of 40 dB when compared to a single airgun, without any increase in peak pressure and a significant reduction in the slope of the pressure. A correction procedure for the effect of the rising bubble was developed, yielding improved correlation between the observed bubble resonance with the well-known Rayleigh-Willis scaling.

The data from the testing indicate that low-pressure high-volume pneumatic sources will provide better low frequency signal and have lower environmental impact compared to high pressure airguns.

Introduction

Low frequencies are very beneficial for seismic exploration. The reasons for this are manifold, e.g. deeper penetration, sharper wavelet, improved QI and reduced cycle skipping in FWI based velocity model building. Generating a seismic signal with good S/N and stable phase in the 1-4 Hz band is a hard problem though both onshore and offshore. After much progress with receivers, the remaining challenge now is seismic sources. This paper describes the testing of a novel marine low frequency source named Tuned Pulse Source (Ronen et al, 2017; Baeten et al, 2019). In this paper, results from a field trial with a large volume (20,600 cubic inch) TPS are described. During this field trial, data were acquired using different firing pressures and source depths. The data show that larger TPS volumes, approximately 100 times the volume of a conventional air gun, deliver significantly more low frequency signal than conventional airguns. After considering bubble rise effects, the bubble periods of these large volume sources are in good agreement with the Rayleigh-Willis relation. In addition to the increase in low frequency signal, the data show that there is a decrease in high frequency content. To reduce environmental impact the TPS was designed to reduce environmental impact by reducing high frequency output.

Field trial description

In August 2019, an experiment using the TPS was performed at a lake test site in Virginia, USA (Figure 1). The purpose of the test was to measure the sound pressure emitted by the TPS, and to compare the TPS output against the output of a conventional airgun for a variety of firing pressures and source depths. The source was deployed by a crane in a stationary position and recordings were made by several hydrophones located approximately 6-10 m away from the source.

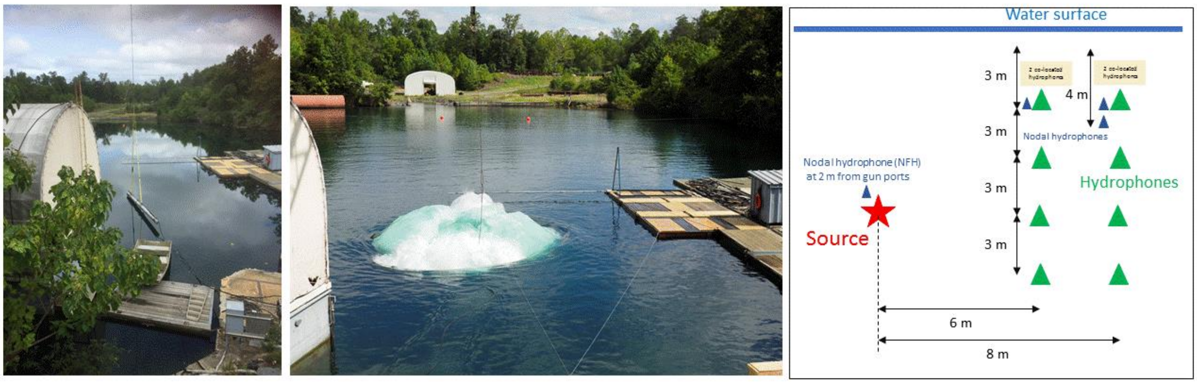

(a) (b) (c)

Figure 1 ***(a)*** *Deploying the 20,600 cui TPS into the lake,* ***(b)*** *bubble due to source firing at 15 m depth,* ***(c)*** *measurement set-up. A total of 12 different hydrophone locations were present during the test.*

TPS versus conventional airgun

A comparison between a conventional 280 cui Bolt airgun and the 20,600 cui TPS was obtained using data recorded at an identical hydrophone position, with the two sources fired at identical location and depth. The only correction that is applied to the raw data is a simple scalar representing the inverse of the distance between gun and hydrophone, to calculate a hydrophone response at 1m from the source. The result is shown in Figure 2. It is observed that the low-frequency output of the TPS gun exceeds the Bolt output by 40 dB at 3 Hz. The signal from the airgun at low frequencies is below ambient noise so no reliable comparison can be made below ~2 Hz. Note that the large improvement in low-frequency content is obtained with a slight decrease in the peak pressure of 4-5 BarM. In addition, the TPS has a longer rise time, leading to a significant reduction in environmental impact.

Near-to-far-field extrapolation

As outlined above, the sound pressure generated by the TPS was measured at various hydrophone locations in the near field, where the source-receiver distance varied between 3 and 15 m.

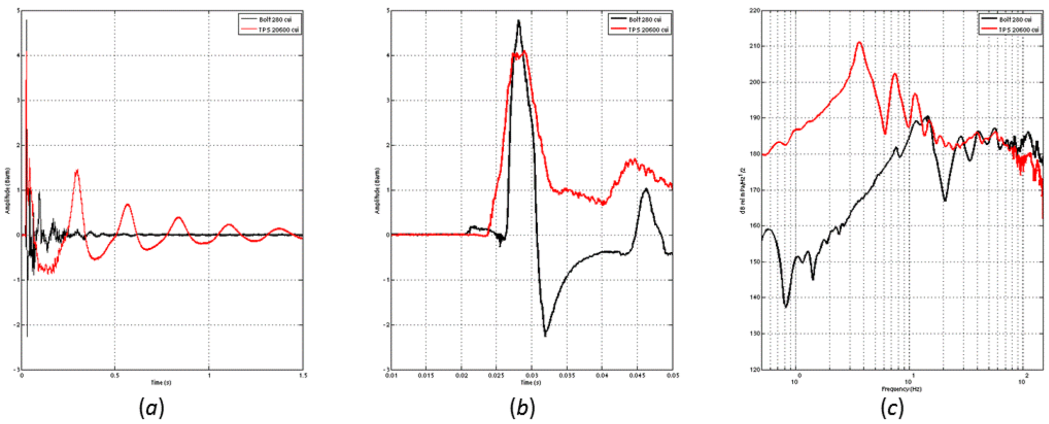

Figure 2. *Data from the same hydrophone showing TPS versus Bolt. (a) time domain. (b) zoom-in of (a), illustrating the difference in rise time. (c) Spectra of the two signals. Note the 40dB (factor 100!) difference in low frequency signal and a slight reduction in peak amplitude from 4.7 to 4 BarM.*

To obtain a standardized TPS performance that allows comparison of the measurements at the various hydrophone locations, we extrapolate the measured data to the far field, by rescaling the amplitudes to mimic a far field signature 1 m vertically below the source ("reference location"). The distance L between source and receiver is equal to $L = [(d_s - d_r)^2 + h^2]^{1/2}$. The distance L_i between image source and receiver is $L_i = [(d_s + d_r)^2 + h^2]^{1/2}$. The phase difference $\delta\varphi$ between the signals that come to the receiver directly from the source and after the reflection from the water surface is equal to $\delta\varphi = k\,(L_i - L\,) + \pi$. Here, $k = 2\pi f/c$, f is the signal frequency, c is the sound speed in water, and the term π accounts for the phase reversal at the water/air interface. Let $\hat{p}_{f,1}$ be the component of the sound pressure with frequency f at one-meter distance from the source. The amplitude of this component at the source position will be $|\hat{p}_{f,s}| = |\hat{p}_{f,1}(1/L + exp(i\delta\varphi)/L_i)|$, where we assume a $1/L$ signal decay with the distance. We use the above equations to remove the surface reflection effect (ghost) in the near field and to apply it in the far field. This gives the relation between the frequency components of the sound pressure $\hat{p}_{f,s}$ measured by the near-field hydrophones and the expected amplitude of these components $\hat{p}_{f,\infty}$ in the far-field directly below the source,

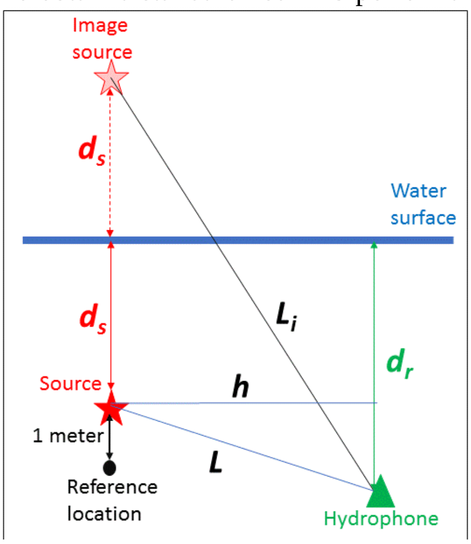

Figure 3 *Nomenclature used in near-to-far-field normalization procedure*

$$|\hat{p}_{f,\infty}|L_\infty = \left|\hat{p}_{f,1}\,\frac{1 + exp(i\delta\varphi_0)}{1/L + exp(i\delta\varphi)/L_i}\right|. \qquad (1)$$

Here, L_∞ is the distance between the source and a far field observation point and $\delta\varphi_0 = 2k\,d_s + \pi$. Equation (1) essentially removes the near field ghost, adds a far field ghost and normalizes to 1 m source receiver distance.

Figure 4 shows the application of deghosting and scaling to data from one of the shots, where the sound pressure was measured by six hydrophones at different positions. The difference between uncorrected, recorded amplitudes of the sound pressure spectrum reaches 10 dB. After the near-to-far-field extrapolation procedure, this difference reduces to 1-2 dB, illustrating the success of this procedure.

Dependence on depth and firing pressure

For each shot, we averaged the extrapolated far-field data over all the records. The averaged far-field extrapolation was used to evaluate the source performance as a function of its depth and firing pressure. Figure 5 *(left)* shows shots at the same pressure of 1,000 psi and volume of 20,600 cui, but at different depths. The bubble frequency and the amplitude decrease with decreasing depth.

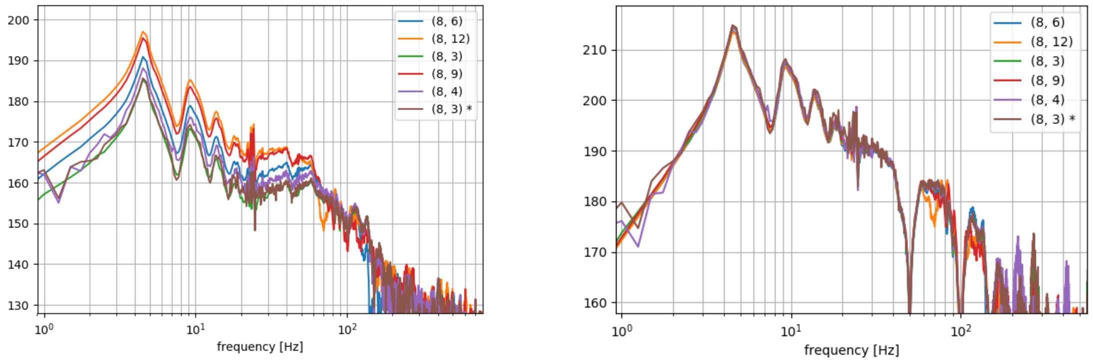

Figure 4 *Spectra of shot at 15 m depth with TPS pressure of 600 psi and volume of 20600 cui. Left: near-field spectrum measured by hydrophones. Right: extrapolation of the measured spectrum to the far field. Numbers in brackets indicate positions of hydrophones as "(horizontal distance to the source, depth)". The star symbol "*" refers to the hydrophone at 3-meter depth (a small triangle in figure 1(c)).*

As a result, only a marginal increase of the low-frequency part of the spectrum is achieved by shooting at shallow depths. One shot at the same pressure and volume was fired at a depth of 3 m. The resulting air-bubble quickly broke the water surface and the generated sound was significantly weaker compared to the other shots. The shots shown in Figure 5 (right) were fired at 15 m depth with a volume of 20,600 cui and varying firing pressure. An increase in the firing pressure reduces the bubble frequency and provides a slight increase in the spectrum at high frequencies.

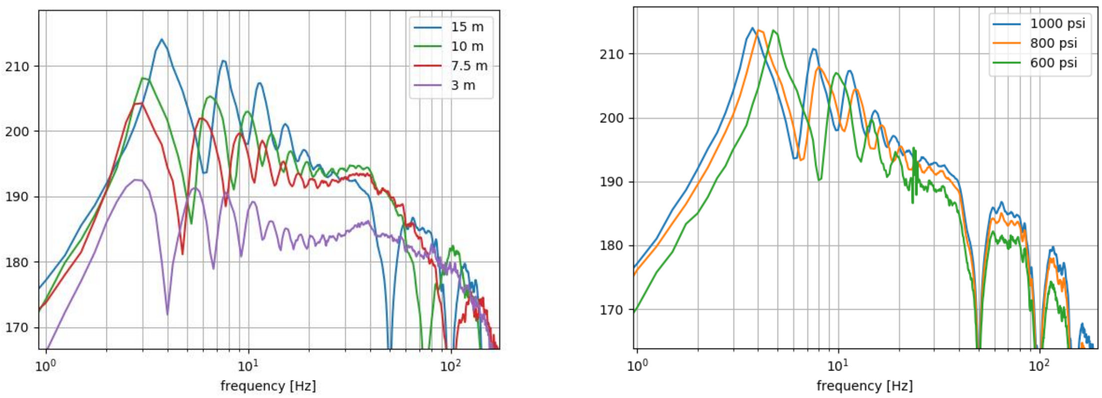

Figure 5 *Dependence of generated sound spectra (dB relative to 1 micro pascal at 1 meter) on source depth (left) and firing pressure (right). The airgun volume is 20600 cui. Left: shots at a pressure of 1000 psi. Right figure shows shots at 15-meter depth. Measured signals have been extrapolated to the far field and averaged over the hydrophone records.*

Period of bubbles oscillations

We have checked the applicability of the Rayleigh-Willis formula for large air-bubbles. According to this formula, the period of bubble oscillations T varies as

$$T = \kappa\, \rho^{1/2} (p_0 V_0)^{1/3} / {p_w}^{5/6}. \qquad (2)$$

Here, ρ is the water density, p_0 and V_0 are source pressure and volume, p_w is the pressure of water at the source depth, and κ is a constant. We followed two approaches to evaluate the oscillation periods of observed bubbles: 1) measuring time intervals between consecutive minima and maxima in the hydrophone data, and 2) calculating T from the relation $T = 1/f_{max}$, where f_{max} is the frequency corresponding to the major peak in the measured sound pressure spectrum. The two approaches give similar estimations of T. Figure 6 (left) compares consecutive time intervals between maxima and minima of measured sound pressures with scaling according to equation (2) where we set $\kappa = 1.8$. Note that after correction for the bubble ascent, the same κ constant applies to both large bubbles from a 20,600 cui TPS and to small bubbles from a 280 cui airgun. For each record we took six such intervals – three intervals between maxima and three intervals between minima. The time intervals between the first and the second maxima characterize the bubble period only approximately, because the first pressure peak appears before a bubble is fully formed. The colour of the dots follows the rainbow pattern and it indicates the succession of intervals. Earlier time intervals, which are shown by the red colour, are in general shorter than later time intervals. The outlier in Figure 6 (left) corresponds to the shot at 3-meter depths, where the bubble quickly broke the water surface.

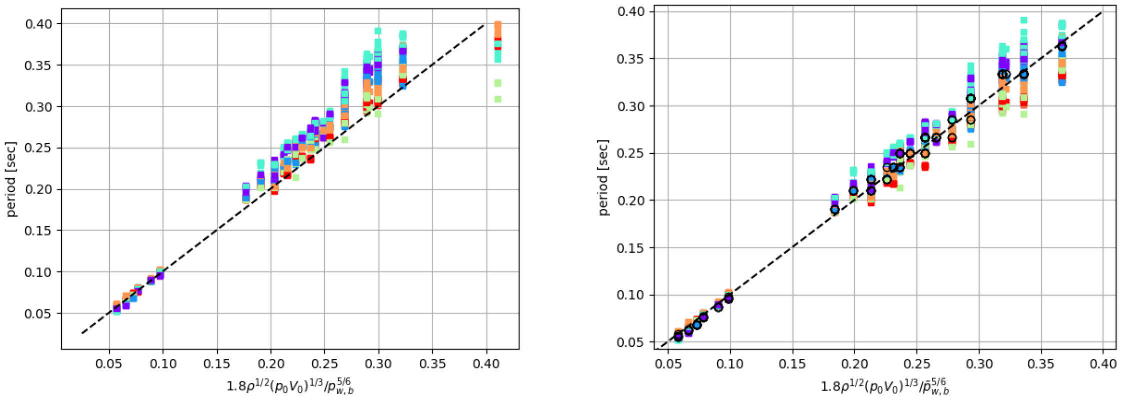

Figure 6 *Comparison of observed bubble periods with Rayleigh-Willis scaling (left) and Rayleigh-Willis scaling corrected for the bubble ascent (right). Dots represent time intervals between four consecutive maxima and minima in hydrophone data. The colour of the dots varies from red for earlier time intervals to indigo for later time intervals. Black circles in the right figure represent values $T = 1/f_{max}$. Dashed black lines are values of T that follow from the Rayleigh-Willis relation (2) (left), and from relation (2) where the pressure $\bar{p}_w$ is calculated at the airgun depth corrected for the bubble ascent (3) (right).*

From Figure 6 (left), one observes that measured periods deviate from the Rayleigh-Willis equation (2) for large bubbles. We expect that this deviation appears because bubbles move up, and they emit sound at a depth which is different from the airgun depth. Larger bubbles rise in average with a higher speed, since the buoyancy force, which pushes the bubbles up, increases faster with the bubble size than the drag force, which slows them down. Most of the sound energy is emitted during the first few bubble cycles. We have estimated the vertical distance δh travelled by the bubble during the first few cycles as

$$\delta h = \kappa_u (\varrho g)^{1/2} \frac{(p_0 V_0)^{1/2}}{p_w} \left(\frac{p_w}{p_0}\right)^{1/12}, \tag{3}$$

where κ_u is a numerical factor. To correct equation (2) for the bubble ascent, we make the substitution $p_w \to \bar{p}_w$, where $\bar{p}_w$ is the ambient water pressure calculated at the depth $d - \delta h$. Figure 6 (right) compares the data acquired with the corrected Rayleigh-Willis relation, where we set $\kappa = 1.8$ and $\kappa_u = 4.0$. The simulated value of δh varies between 2 and 3.8 meters for TPS shots.

Conclusions

We have successfully tested a new marine source whose initial volume of up to 100 times the volume of a conventional airgun produces low-frequency bubble oscillations with a resonance in the order of 3 Hz. The resulting improvement in low frequency output is in the order of 40 dB when compared to a single airgun, without any increase in peak pressure and a significant reduction in the slope of the pressure. A correction procedure for the effect of the rising bubble was developed, yielding improved correlation between the observed bubble resonance with the well-known Rayleigh-Willis scaling.

The data from the testing indicate that low-pressure high-volume pneumatic sources will provide better low frequency signal and have lower environmental impact compared to high pressure airguns.

References

Ronen, S. and Chelminski, S. [2017] Tuned Pulse Source – a new low frequency seismic source. *87th SEG Annual Meeting*, Expanded Abstracts, 6085-6088.

Baeten, G., Chavan, D., Kuvshinov, B., Ten Kroode, F., Ronen, S., Chelminski, S. and Chelminski, J. [2019] A marine seismic source with enhanced low and reduced high frequency content. *81st EAGE Conference and Exhibition*, Extended Abstract